Analyst

COMMUNICATION

Cite this: *Analyst*, 2015, **140**, 7854

Received 28th September 2015,
Accepted 13th October 2015

DOI: 10.1039/c5an01998b

www.rsc.org/analyst

Real-time reaction monitoring by ultrafast 2D NMR on a benchtop spectrometer†

Boris Gouilleux,[a] Benoît Charrier,[a] Ernesto Danieli,[b] Jean-Nicolas Dumez,[c] Serge Akoka,[a] François-Xavier Felpin,[a,d] Mireia Rodriguez-Zubiri[a] and Patrick Giraudeau*[a,d]

Reaction monitoring is widely used to follow chemical processes in a broad range of application fields. Recently, the development of robust benchtop NMR spectrometers has brought NMR under the fume hood, making it possible to monitor chemical reactions in a safe and accessible environment. However, these low-field NMR approaches suffer from limited resolution leading to strong peak overlaps, which can limit their application range. Here, we propose an approach capable of recording ultrafast 2D NMR spectra on a compact spectrometer and of following in real time reactions in the synthetic chemistry laboratory. This approach – whose potential is shown here on a Heck–Matsuda reaction – is highly versatile; the duration of the measurement can be optimized to follow reactions whose time scale ranges from between a few tens of seconds to a few hours. It makes it possible to monitor complex reactions in non-deuterated solvents, and to confirm in real time the molecular structure of the compounds involved in the reaction while giving access to relevant kinetic parameters.

Introduction

Reaction monitoring based on analytical spectroscopy provides essential kinetic and speciation information in a variety of application fields, from organic and inorganic synthesis to biochemistry and bioengineering.[1,2] It is therefore a determining tool to deeply understand reaction mechanisms. The development of accessible, powerful and robust analytical methods is highly important to characterize in real time the molecular compounds involved in such processes. Among spectroscopic techniques, NMR has the great advantage of being non-specific and non-destructive; it does not require prior knowledge of the analyzed compounds and delivers both structural and quantitative information. High field NMR (HF NMR) has been widely used in organic and pharmaceutical applications for monitoring chemical processes, either directly inside the NMR tube[3–5] or by using flow cells.[6–10]

Yet, the high analytical performance of HF NMR is associated with expensive instrumentation, high monetary and environmental cost, and the need for specific facilities which are barely compatible with the working environment of the synthetic chemistry laboratory, in contrast with other techniques such as UV Vis, FTIR or Raman spectroscopy. However, low field NMR (LF NMR) spectroscopy has recently been brought under the hood through the development of a new generation of benchtop spectrometers relying on non-cryogenic magnets. These spectrometers have the advantage of being relatively inexpensive, practical, transportable and eco-friendly. During the last few years, the quality of the ^{1}H spectra recorded with these compact spectrometers has been greatly improved, particularly in terms of sensitivity and stability. These developments have enabled the successful application of benchtop NMR to monitor reactions "on the fly".[11–13] However, LF NMR suffers from intrinsic drawbacks *vis-à-vis* its HF counterpart, particularly in terms of low spectral resolution. The low magnetic field inevitably leads to a reduced dispersion of frequencies, generating numerous peak overlaps. Moreover, the real-time identification of chemical compounds is further complicated by the strong couplings commonly encountered in LF NMR. So far, resolution losses and peak overlap have limited the application range of LF NMR to the monitoring of relatively simple reactions where the peaks of interest are well isolated.

2D NMR experiments[14,15] are well-known to offer an efficient way of discriminating resonances while delivering invaluable structural information. A number of 2D pulse-sequences have already been developed on some benchtop spectrometers to take advantage of this methodology at low

[a]*CEISAM CNRS, UMR6230, Université de Nantes, BP 92208, 2 rue de la Houssinière, 44322 Nantes, France. E-mail: patrick.giraudeau@univ-nantes.fr*
[b]*Institut für Technische und Makromolekulare Chemie (ITMC), RWTH Aachen University, Worringerweg 1, 52074 Aachen, Germany*
[c]*CNRS UPR2301, Institut de Chimie des Substances Naturelles, 1 avenue de la Terrasse, 91198 Gif-sur-Yvette Cedex, France*
[d]*Institut Universitaire de France, 1 rue Descartes 75005, Paris Cedex 05, France*
† Electronic supplementary information (ESI) available: Experimental procedures and parameters. See DOI: 10.1039/c5an01998b

field.[12] Unfortunately 2D NMR is affected by a long acquisition duration, arising from the need to sample the indirect dimension through the repetition of numerous experiments. As a fundamental consequence, conventional 2D NMR is not adapted to study samples whose composition evolves in the course of time,[16] unless time-resolved schemes based on non-uniform sampling (NUS) are employed.[17] In this context, ultrafast (UF) NMR, which is capable of acquiring 2D spectra within a single scan,[18] offers an attractive way to circumvent this drawback. Therefore, the implementation of UF NMR on a benchtop spectrometer would be a powerful analytical tool to monitor chemical reactions directly inside the synthetic chemistry laboratory and in real time. While UF NMR is now recognized as a powerful reaction monitoring tool at high field,[16,19–24] it has never been reported on a benchtop spectrometer, as it requires specific hardware. In fact, UF experiments rely on a spatial encoding scheme, which is also used in many other liquid-state NMR experiments, but has never been shown at low field.

In this article, we report the first spatially encoded NMR experiment on a compact benchtop spectrometer, using a permanent magnet based on a Hallbach design.[25,26] This spectrometer includes a gradient coil along the B_0-axis which is efficient enough to meet the criteria to implement the UF methodology. Thanks to this device, the first UF spectra recorded on a benchtop spectrometer are shown, and the promising potential of this new analytical tool is demonstrated on the real-time monitoring of a Heck–Matsuda coupling reaction,[27] through UF COSY spectra recorded in real time during the chemical process.

Results and discussion

First UF spectra on a benchtop NMR spectrometer

The UF approach relies on the design of a spatially dependent evolution period. In order to perform this spatial encoding, a magnetic field gradient – applied together with frequency-swept pulses – is necessary to induce a position-dependent resonance frequency, and also to refocus spatially encoded magnetization during a detection scheme based on echo-planar spectroscopic imaging (EPSI).[28] The benchtop product (designed by Magritek, Aachen, Germany, a version of the commercial Spinsolve benchtop spectrometer) includes a gradient coil designed for pulsed-gradient spin echo diffusion measurements. By implementing an appropriate pulse sequence, this gradient coil provides a robust and strong enough magnetic field gradient to achieve these UF features. Here, we implemented and optimized a constant-time and phase-modulated spatial encoding pulse sequence based on a double spin echo scheme.[29] A combination of bipolar gradients based on EPSI was also implemented during the detection period. Further information about the pulse-sequence and detailed parameters are available in the ESI.†

As a proof of concept, we acquired an initial UF COSY spectrum in 400 ms on a model sample at 43 MHz (Fig. 1B). The quality of this spectrum and the good match with the expected spectrum (numerical simulation[30] shown in Fig. 1C) highlight the suitability of UF experiments at low field and the technical performance of the benchtop prototype. As the value of coupling constants is not negligible compared to the resolution, the coupling-patterns are visible along the vertical dimension for the low-field spectrum (Fig. 1B and C), while they are not observed at 400 MHz (Fig. 1E and F).

The comparison of 1D (Fig. 1A and B) and 2D spectra (Fig. 1D and E) at low and high fields shows that field-induced resolution losses are far less important for UF COSY experiments than for 1D pulse-acquire ^{1}H spectra. This is mainly explained by the fact that the UF experiments used in the present study, which are based on a "constant-time" encoding, are intrinsically decoupled along the horizontal (or ultrafast) dimension,[31] *i.e.*, they are "singly pure-shift" sequences.[32] Thanks to this feature, UF experiments provide a valuable discrimination of resonances at low field. The major drawback is the relatively low sensitivity, since the experimental limit of detection (LOD) decreases from typically 0.1 mol L^{-1} at 400 MHz (ref. 19) to 1 mol L^{-1} at 43 MHz for a one scan acquisition. However, this sensitivity loss is far less critical than what could be expected from the difference of one order of magnitude between magnetic fields. This is due in part to the probe design, but also to the fact that UF experiments are characterized by the need to compromise between resolution, sensitivity and spectral width.[19] At low field, the spectral widths are much smaller, which considerably alleviates this compromise. Still, the single-scan limit of detection is quite high, but when the timescale of the targeted reaction is compatible with acquisition duration between a few seconds and a few minutes, the single-scan LOD can be increased by signal averaging while avoiding t_1-noise. This hybrid approach has shown great potential at high field for a variety of applications.[33] A detailed evaluation of the analytical performance of UF experiments at low field will be carried out in further studies.

Real-time reaction monitoring by UF NMR

We evaluate here the potential of benchtop UF 2D NMR through the monitoring of a Pd-catalyzed Heck–Matsuda reaction[27] (Fig. 2A). This variant of the Heck coupling uses aryl diazonium salts as highly reactive aryl halide surrogates and allows reaction at room temperature under ligand- and base-free conditions.[34] The Heck–Matsuda reaction has recently found a growing interest among the synthetic community,[35–39] especially since their hazardous character was overcome by a bicatalytic strategy[40,41] or a continuous-flow approach.[42,43]

The sequential diazonium formation–coupling reaction, depicted in Fig. 2A, is performed directly inside an NMR tube with an initial concentration of 0.36 mol L^{-1} for the limiting starting material: 4-methyl-2-nitroaniline (**1**). In this reaction, the aniline (**1**) dissolved in methanol first reacts with *t*-BuONO and $MeSO_3H$ to form a diazonium salt. The latter is then coupled with the olefin (**2**) in the presence of $Pd(OAc)_2$ as the catalyst, in order to produce the styrene (**3**). The experiment was designed to keep the mixture as homogeneous as possible

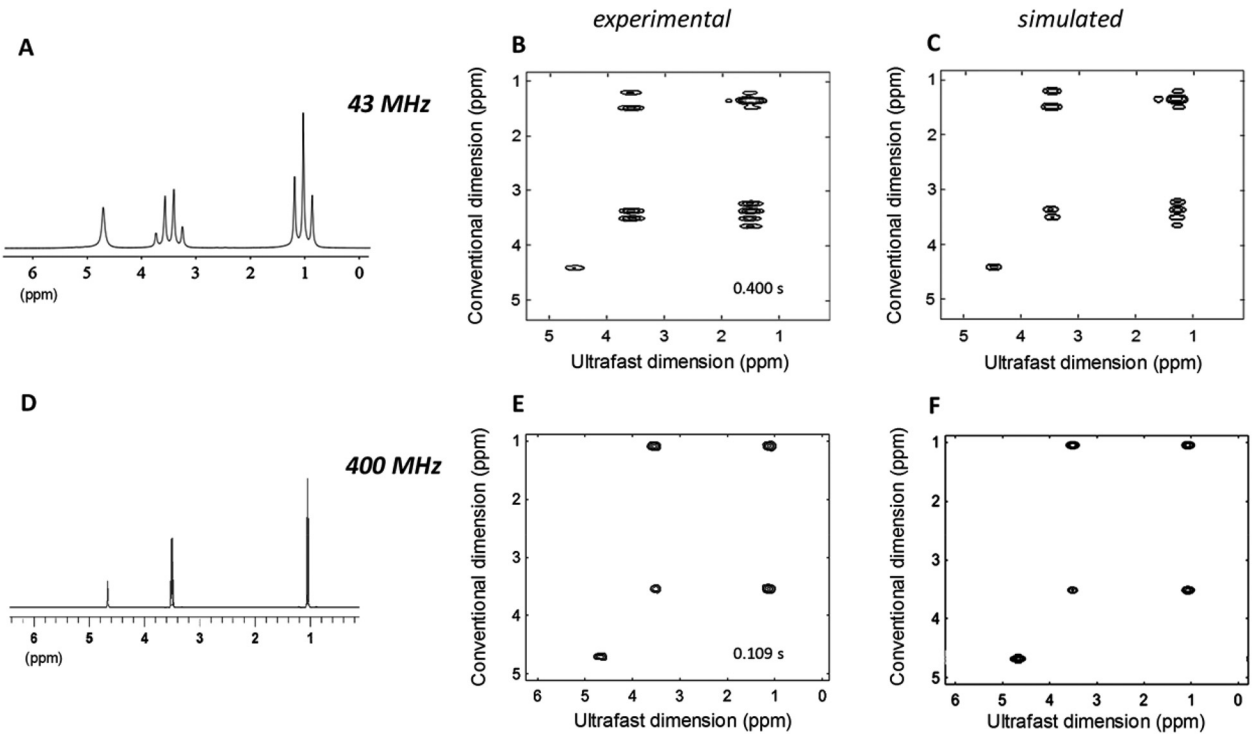

Fig. 1 Comparison of low-field and high-field ultrafast 2D and 1D spectra on a model sample. Top line: 1D ^{1}H spectrum (A), experimental (B), and simulated (C) UF COSY spectra obtained at 43 MHz. Bottom line: same spectra obtained at high field (400 MHz) (D–F). All the experimental spectra were recorded on a sample of ethanol in D_2O (40/60: v/v). The "ultrafast" axis refers to the spatially encoded dimension (without Fourier transformation) whereas the "conventional" axis represents the direct dimension. The simulations (C and F) were performed thanks to a simulation platform that we recently introduced.[30]

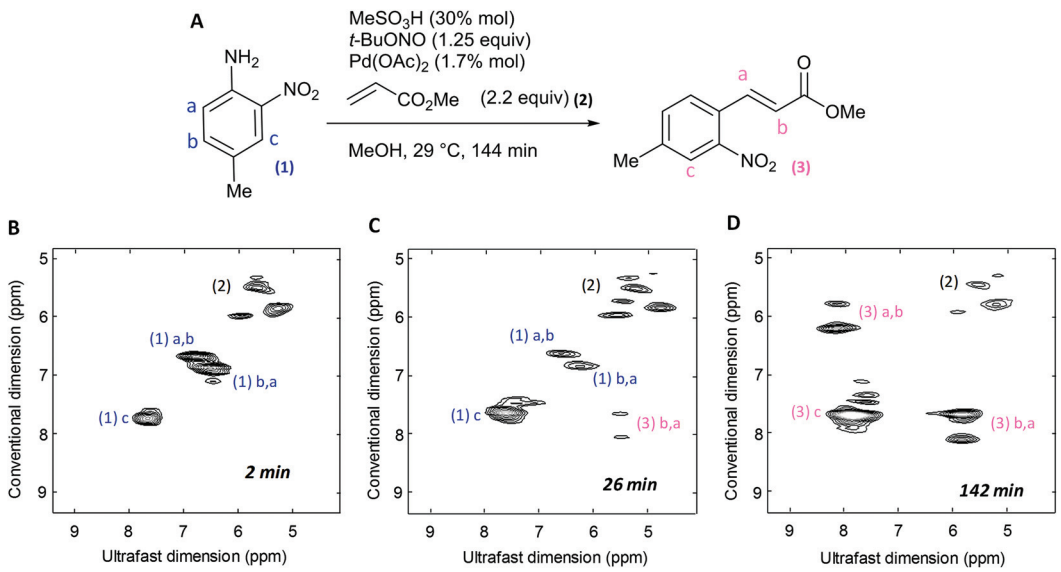

Fig. 2 Scheme of the one pot Heck–Matsuda reaction in the multicomponent mode (A). The reaction was followed for 144 min with an initial concentration of 0.36 mol L^{-1} for the limiting starting material (1), at 29 °C directly inside the NMR tube. The reaction was monitored through 55 UF COSY spectra recorded with 36 scans every 2.6 minutes, for instance: at 2 min (B), 26 min (C), and 142 min (D). Peak assignments are also indicated.

(the detailed procedure is available in the ESI†). It is important to note that thanks to an external lock system, our experiments were carried out in a non-deuterated solvent. This reduces the cost of the monitoring and allows us to avoid unwanted potential isotopic effects that could affect reaction rates in deuterated solvents.

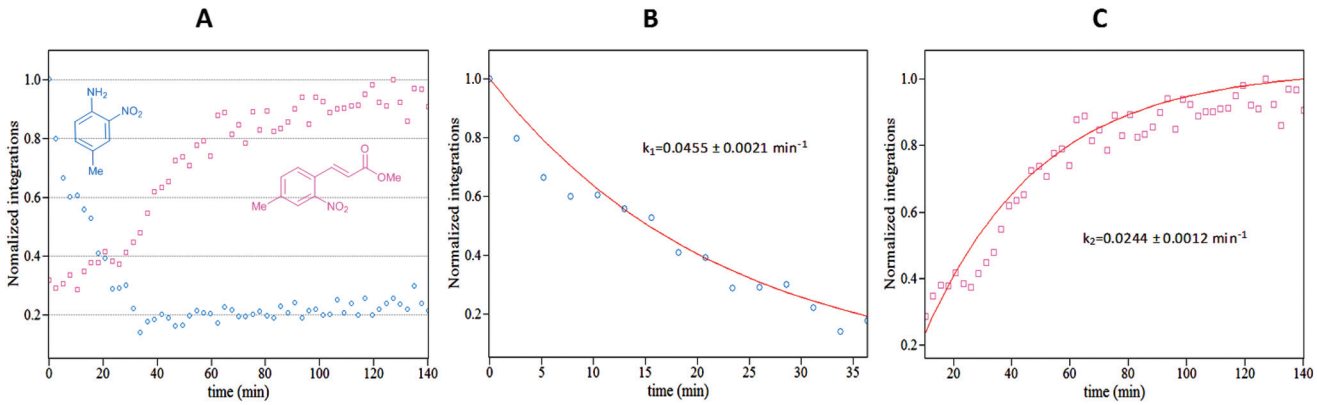

Fig. 3 Kinetics from the reaction monitoring (A) showing the evolution of normalized 2D peak volumes as the reaction progresses. These volumes were calculated from the cross-peaks (1) a,b and (3) b,a indicated in Fig. 2, corresponding to the starting material and the final product, respectively. Blue open circles show the consumption of aniline and the pink open squares show the formation of the final styrene. The curves were obtained thanks to 55 UF COSY spectra recorded every 2.6 min. Kinetic constants can be extracted through exponential fitting of the 2D peak volumes in the relevant time domains, *i.e.* from 0 to 40 min for the consumption of aniline (B) and from 20 to 140 min for the production of the final styrene (C).

UF COSY spectra are well-suited to monitor in real time this chemical reaction, as they deliver well-resolved cross-peaks, both for the product (**3**) and for the limiting starting material (**1**) (Fig. 2C–E). The starting material in excess (**2**) is also visible. Note that the reaction could not be studied through 1D spectra because the reactant and product peaks were overlapped between them and with the strong non-deuterated solvent peak. In order to optimize the sensitivity of the targeted peaks relative to the reaction time scale, the number of scans was set to 36 with a recovery time of $1.25 \cdot T_1$,[44] leading to the acquisition of a COSY spectrum every 2.6 min. In addition, *J*-modulation effects, arising from the constant-time nature of the spatial encoding, play a central role in the sensitivity and can be predicted thanks to numerical simulations.[30] These effects were therefore finely tuned for the cross-peaks of interest by adjusting the total time spent in the transverse plane. In this procedure, the sensitivity was optimized simultaneously for the limiting reactant (**1**) and the product (**3**). The reactant in excess was not considered in this optimization. The kinetic curves recorded from the time-evolution of 2D peak volumes are shown in Fig. 3A. These curves depict the two chemical processes involved in the reaction very well. The decreasing blue curve matches with the initial conversion of (**1**) into a diazonium salt. After the aniline is consumed (at *ca.* 20 min), the coupling reaction starts, leading to the final styrene (**3**) (increasing pink curve). Relevant kinetic parameters, namely the rate constants of the two consecutive processes, can be extracted thanks to a mono-exponential fitting of the corresponding time-domain data (Fig. 3B and C). The trend of the curves and the rate constants reveal that the coupling reaction is the rate-limiting step of the process with respect to the diazonium formation. From a qualitative point of view, this result is consistent with previous studies performed at high-field,[42] which highlight that the use of an electron-poor aniline leads to a quick conversion into a diazonium salt, thereby making the coupling process the rate-limiting step.

Conclusions

This paper demonstrates the potential of benchtop ultrafast 2D NMR. This new analytical approach extends the reaction monitoring toolkit for a broad community of synthetic chemists, making real-time 2D NMR directly available under the fume hood. When concentration allows it, the duration of the 2D measurement can be optimized to follow reactions whose timescale ranges from a few tens of seconds to a few hours. The ability of UF 2D NMR to discriminate overlapping resonances is particularly valuable at low field where the frequency dispersion is significantly reduced. From the NMR point of view, this first report of spatially encoded NMR experiments on a benchtop spectrometer could open the way to a number of developments for in-lab analysis of liquid-state samples, including other homo- or heteronuclear UF pulse sequences, pure-shift experiments or diffusion-based measurements. In particular, heteronuclear pulse sequences would give access to larger numbers of a correlation peaks, thus making more complex reactions accessible. The potential and the suitability of UF NMR on a benchtop spectrometer have been shown through the real-time monitoring of a Heck–Matsuda reaction, leading to kinetic results which are consistent with the literature. This first application could open the way to a broad range of applications in synthetic chemistry, including the on-flow monitoring of chemical processes, a research avenue that we will explore in the near future.

Acknowledgements

The authors warmly acknowledge Magritek, in particular Juan Perlo and Andrew Coy, for their strong support. We also thank Nicolas Oger and Laetitia Rouger (CEISAM) and Stefano Caldarelli (ICSN) for discussions, as well as Michel Giraudeau for linguistic assistance. This project was funded by Région

Pays de la Loire (Grant RésoNantes). ED acknowledges financial support from Deutsche Forschungsgemeinschaft (DFG Gerätezentrum Pro2NMR).

Notes and references

1 J. Workman, M. Koch and D. Veltkamp, *Anal. Chem.*, 2007, **79**, 4345–4364.
2 J. Workman, M. Koch, B. Lavine and R. Chrisman, *Anal. Chem.*, 2009, **81**, 4623–4643.
3 F. Susanne, D. S. Smith and A. Codina, *Org. Process Res. Dev.*, 2012, **16**, 61–64.
4 I. M. Clegg, C. M. Gordon, D. S. Smith, R. Alzaga and A. Codina, *Anal. Methods*, 2012, **4**, 1498–1506.
5 T. R. Hoye, B. M. Eklov, T. D. Ryba, M. Voloshin and L. J. Yao, *Org. Lett.*, 2004, **6**, 953–956.
6 M. Maiwald, H. H. Fischer, Y.-K. Kim, K. Albert and H. Hasse, *J. Magn. Reson.*, 2004, **166**, 135–146.
7 M. A. Bernstein, M. Štefinović and C. J. Sleigh, *Magn. Reson. Chem.*, 2007, **45**, 564–571.
8 M. Khajeh, M. A. Bernstein and G. A. Morris, *Magn. Reson. Chem.*, 2010, **48**, 516–522.
9 A. C. Barrios Sosa, R. T. Williamson, R. Conway, A. Shankar, R. Sumpter and T. Cleary, *Org. Process Res. Dev.*, 2011, **15**, 449–454.
10 D. A. Foley, C. W. Doecke, J. Y. Buser, J. M. Merritt, L. Murphy, M. Kissane, S. G. Collins, A. R. Maguire and A. Kaerner, *J. Org. Chem.*, 2011, **76**, 9630–9640.
11 S. K. Küster, E. Danieli, B. Blümich and F. Casanova, *Phys. Chem. Chem. Phys.*, 2011, **13**, 13172–13176.
12 V. Sans, L. Porwol, V. Dragone and L. Cronin, *Chem. Sci.*, 2015, **6**, 1258–1264.
13 M. V. Silva Elipe and R. R. Milburn, *Magn. Reson. Chem.*, 2015, DOI: 10.1002/mrc.4189.
14 W. P. Aue, E. Bartholdi and R. R. Ernst, *J. Chem. Phys.*, 1976, **64**, 2229–2246.
15 J. Jeener, Lecture presented at Ampere International Summer School II, Basko Polje, Yugoslavia, 1971.
16 R. Boisseau, U. Bussy, P. Giraudeau and M. Boujtita, *Anal. Chem.*, 2015, **87**, 372–375.
17 R. Dass, W. Koźmiński and K. Kazimierczuk, *Anal. Chem.*, 2015, **87**, 1337–1343.
18 L. Frydman, T. Scherf and A. Lupulescu, *Proc. Natl. Acad. Sci. U. S. A.*, 2002, **99**, 15858–15862.
19 P. Giraudeau and L. Frydman, *Annu. Rev. Anal. Chem.*, 2014, **7**, 129–161.
20 A. Herrera, E. Fernández-Valle, R. Martínez-Álvarez, D. Molero, Z. D. Pardo, E. Sáez and M. Gal, *Angew. Chem., Int. Ed.*, 2009, **48**, 6274–6277.
21 A. Herrera, E. Fernandez-Valle, E. M. Gutiérrez, R. Martinez-Alvarez, D. Molero, Z. D. Pardo and E. Saez, *Org. Lett.*, 2010, **12**, 144–147.
22 L. H. K. Queiroz Junior, P. Giraudeau, F. A. B. dos Santos, K. T. Oliveira and A. G. Ferreira, *Magn. Reson. Chem.*, 2012, **50**, 496–501.
23 Z. D. Pardo, G. L. Olsen, M. E. Fernández-Valle, L. Frydman, R. Martínez-Álvarez and A. Herrera, *J. Am. Chem. Soc.*, 2012, **134**, 2706–2715.
24 A. Herrera, E. Fernández-Valle, R. Martínez-Álvarez, D. Molero-Vílchez, Z. D. Pardo-Botero and E. Sáez-Barajas, *Magn. Reson. Chem.*, 2015, **53**, 952–970.
25 E. Danieli, J. Perlo, B. Blümich and F. Casanova, *Angew. Chem., Int. Ed.*, 2010, **49**, 4133–4135.
26 E. Danieli, J. Perlo, B. Blümich and F. Casanova, *Phys. Rev. Lett.*, 2013, **110**, 180801.
27 K. Kikukawa and T. Matsuda, *Chem. Lett.*, 1977, **6**, 159–162.
28 P. Mansfield and P. G. Morris, *NMR imaging in biomedicine*, Academic Press, New-York, 1982.
29 P. Pelupessy, *J. Am. Chem. Soc.*, 2003, **125**, 12345–12350.
30 B. Gouilleux, L. Rouger, C. Benoît, I. Kuprov, S. Akoka, J.-N. Dumez and P. Giraudeau, *ChemPhysChem*, 2015, **16**, 3093–3100.
31 P. Giraudeau and S. Akoka, *J. Magn. Reson.*, 2008, **192**, 151–158.
32 R. W. Adams, L. Byrne, P. Kiraly, M. Foroozandeh, L. Paudel, M. Nilsson, J. Clayden and G. A. Morris, *Chem. Commun.*, 2014, **50**, 2512–2514.
33 S. Akoka and P. Giraudeau, *Magn. Reson. Chem.*, 2015, **53**, 986–994.
34 F.-X. Felpin, K. Miqueu, J.-M. Sotiropoulos, E. Fouquet, O. Ibarguren and J. Laudien, *Chem. – Eur. J.*, 2010, **16**, 5191–5204.
35 F.-X. Felpin, L. Nassar-Hardy, F. Le Callonnec and E. Fouquet, *Tetrahedron*, 2011, **67**, 2815–2831.
36 N. Oger, M. d'Halluin, E. Le Grognec and F.-X. Felpin, *Org. Process Res. Dev.*, 2014, **18**, 1786–1801.
37 A. Roglans, A. Pla-Quintana and M. Moreno-Mañas, *Chem. Rev.*, 2006, **106**, 4622–4643.
38 J. G. Taylor, A. V. Moro and C. R. D. Correia, *Eur. J. Org. Chem.*, 2011, 1403–1428.
39 F. Mo, G. Dong, Y. Zhang and J. Wang, *Org. Biomol. Chem.*, 2013, **11**, 1582–1593.
40 F. L. Callonnec, E. Fouquet and F.-X. Felpin, *Org. Lett.*, 2011, **13**, 2646–2649.
41 N. Oger, F. Le Callonnec, D. Jacquemin, E. Fouquet, E. Le Grognec and F.-X. Felpin, *Adv. Synth. Catal.*, 2014, **356**, 1065–1071.
42 N. Oger, E. Le Grognec and F.-X. Felpin, *J. Org. Chem.*, 2014, **79**, 8255–8262.
43 N. Oger, E. Le Grognec and F.-X. Felpin, *Org. Chem. Front.*, 2015, **2**, 590–614.
44 P. Schanda, *Prog. Nucl. Magn. Reson. Spectrosc.*, 2009, **55**, 238–265.

